

Saliency-based segmentation of dermoscopic images using color information

Giuliana Ramella

National Research Council, Institute for the Application of Calculus, Italy;
giuliana.ramella@cnr.it

Saliency-based segmentation of dermoscopic images using color information

Skin lesion segmentation is one of the crucial steps for an efficient non-invasive computer-aided early diagnosis of melanoma. In this paper, we investigate how saliency and color information can be usefully employed to determine the lesion region. Unlike most existing saliency-based methods, to discriminate against the skin lesion from the surrounding regions we enucleate some properties related to saliency and color information and we propose a novel segmentation process using binarization coupled with new perceptual criteria based on these properties. To refine the accuracy of the proposed method, the segmentation step is preceded by a pre-processing aimed at reducing the computation burden, removing artifacts, and improving contrast. We have assessed the method on two public databases including 1497 dermoscopic images and compared its performance with that of classical saliency-based methods and with that of some more recent saliency-based methods specifically applied to dermoscopic images. Results of qualitative and quantitative evaluations of the proposed method are promising as the obtained skin lesion segmentation is accurate and the method performs satisfactorily in comparison to other existing saliency-based segmentation methods.

Keywords: Dermoscopic images; Skin lesion; Color image processing; Segmentation; Saliency map; Human visual perception

1. Introduction

Early diagnosis is a determining factor for the prognosis of melanoma since it allows treating this skin cancer at the initial stage through surgical eradication of the cancerous cells with a high cure rate. The common medical practice of melanoma diagnosis is the visual inspection by the dermatologist which, however, has limited accuracy. Several studies [1, 2] have shown that a dermoscopic technique - like solar scan, epiluminescence microscopy, and side transillumination [3-5] – able to display morphological features which are not perceptible by the naked eye, may improve the diagnostic sensitivity of the visual examination by 20–30%.

On the other hand, the skin lesion medical investigation depends heavily on subjective judgment and is not easily reproducible. In particular, the visual inspection of skin lesions in dermoscopic images requires adequate practice. It has been proved that the diagnostic accuracy may be lowered by dermoscopy in case of untrained dermatologists. So, although the subjective expertise of the dermatologist is an extremely important part of the diagnosis process, new and innovative fully automatic methods for segmentation, feature extraction and classification of dermoscopic images can effectively support the skin specialists to perform a faster and more exact skin analysis able to improve the diagnostic assessment process and to make sure of a reliable diagnosis [6-9].

To reduce the aforementioned problems related to the melanoma diagnosis, medical

diagnostic techniques, e.g. the 3-point or 7-point checklist, the Menzies' method, the ABCD rule, and the CASH algorithm [1, 2, 10], are employed in many automatic methods.

Skin lesion segmentation is the first stage in the computerized approach of melanoma diagnosis and is especially relevant due to its hit/effect on the performance of the later steps, i.e. feature extraction and classification. To segment (classify) skin lesion accurately, color information plays an important role since the colors of melanin, the most important chromophore in new tumours visible only by appropriate instrumentation, basically depend on their localization in the skin [1, 11-14]. Indeed, color is regarded by the dermatologists to be one of the major features to discriminate harmful and harmless lesions according to the above dermoscopic rules.

Color image segmentation is itself a complex task and a wide literature exists on this topic [11, 15]. When color image segmentation is applied to dermoscopic images the problem at hand becomes hard to manage since the imaging conditions are frequently inconsistent [16]. In particular, the images can be acquired under different illumination conditions and may have poor resolution. An additional complex problem is related to the presence of artifacts, such as bubbles, hair, shadows, reflections, which may negatively affect and disrupt the analysis of the skin lesions. As a consequence, almost all dermoscopic image segmentation methods include a pre-processing step aimed at improving the quality of the image and at removing the effects of artifacts/aberrations. This step is typically based on standard image analysis techniques such as median filtering [17], color correction [18], illumination correction [19], contrast enhancement [20], and hair removal [21]. Any residual effects should then be suitably considered during the segmentation phase to disrupt as little as possible the skin lesion detection. Also, a post-processing step, mostly based on region merging and/or morphological operations, is often given for the improvement of skin lesion region detection.

Several different methods have been proposed to effectively segment skin lesions [9, 10, 22-24]. The existing methods can be broadly classified as clustering [25], thresholding [26], active contour models [27], region-based [28], and supervised learning [29]. To obtain maximum accuracy, these methods can be applied also in combination [22]. Recently, good results have been obtained by using supervised learning approaches such as convolutional neural networks (CNNs) that, however, require extensive learning based on a very large number of parameters and of labeled training images [29]. Interesting results have been obtained also by region-based methods that employ the saliency to identify relevant regions as those that are visually more distinctive due to their contrast [17, 30-36].

The main drawback of most existing saliency-based methods is because color information is disregarded as the perceptual saliency is computed by localizing the high contrast and brightness region between the background and the foreground of the skin lesion. Some saliency-based methods not specifically designed for skin lesion segmentation using also color information have been proposed [37-39], while the number of skin lesion segmentation methods using saliency and color information remains limited [40]. Since the color information missing is showed by dermatologists as a key factor in the skin lesion detection and evaluation [1, 11-14], by following this recent research direction [40], we propose a new way to employ the saliency, calculated by any valid existing method, along

with the color information of the detected salient region, by resorting to a set of perceptual criteria, describing the lesion, based on saliency and color properties. More detail is available in section 3.

Thus, the main contribution of this work relies on the investigation of how saliency and color information can be usefully employed for skin lesion segmentation. Specifically, we propose a method which besides saliency looks also at the color information, believed as extremely important, to detect the lesion area more exactly. The method consists of a pre-processing step aimed at preparing the image and a successive segmentation process to identify the skin lesion in terms of visual appearance (saliency) and color. The pre-processing step, including the saliency computation, is based on existing methods, while the segmentation step is completely new and constitutes the core of the proposed method. The segmentation process is independent of how the saliency and other preliminary computations (resizing, color reduction, etc.) are computed in the pre-processing step. To give evidence to this aspect we adopt different preliminary computation methods [13, 37-38, 41-43] and we evaluate the corresponding experimental results.

The innovative elements of segmentation step (see section 3) are a) the iterative delineation of the initial salient regions (see step B1.1 in section 3); b) the property of “color proximity”, the definition of peripheral component and the property of “kernel proximity” on which suitable selection criteria are based (see step B1.2 in section 3); c) a criterion based on saliency and color information to manage the case where the foreground/background transition of the skin lesion is not sharp (see step B1.2 in section 3) the segmentation process is extendable since besides saliency and color other types of information can be considered and multiple criteria can be entered.

Here, we extend and improve the preliminary version of the proposed method [14] also by employing it as a sort of baseline to test the effects produced by different methods in the pre-processing step for the computation related to saliency and color. In the following, this new version is referred to as Saliency and Color Segmentation (SCS). Moreover, the method is extensively evaluated for different parameterizations and different methods in the pre-processing step. A further contribution of this paper includes a detailed quantitative and qualitative analysis of the obtained results on two publicly available databases PH2 [44] and ISIC2016 [45], usually used in dermoscopic image processing.

The experimental results confirm a) the effectiveness and the utility of the employment of saliency and color information for skin lesion segmentation; b) SCS is not influenced by the choice of the methods employed in the pre-processing step; c) SCS achieves good quantitative results with an adequate balance and has a competitive and satisfactory performance concerning other existing saliency-based methods; d) SCS implementation is simple and rather fast. It does not require large computational power based on a very large number of parameters and of labeled training images.

The paper is organized as follows. In section 2, we outline the related work, we describe briefly the considered saliency-based methods in the experimental phase and we motivate the choice to use color information together with saliency. In section 3, we describe the method SCS, detailing its main steps and the adopted perceptual criteria also by examples. In section 4, we provide a quantitative and qualitative evaluation of experimental results, also

highlighting the pros and cons. Finally, discussion and conclusions are drawn in section 5.

2. Related work and motivations

Automatic skin lesion segmentation has received great attention in the past decades and in the recent literature, where many segmentation methods based on different approaches can be found. The main advantages and limits of each method have been discussed in many papers [9, 22-24, 46].

Here we focus our attention on the category of region-based methods that typically detect the lesion components (regions) by image processing techniques such as, for instance, statistical region merging [28], modified JSEG [47], watershed [48] and complex networks [49]. More than that, we limit to consider the class of saliency-based methods. This is why saliency has come out as an important tool for medical image analysis since it focuses on the parts of an image that carry useful information according to human visual perception.

Classical saliency-based methods [30-32], that are attributable to the region-based category, have found wide application in image segmentation. In [30], relevance to the given seeds or queries are employed to define the saliency of the image elements (pixels or region). Then, the similarity of image elements with foreground/background cues via the graph-based manifold is ranked and the image is represented by a close-loop graph with superpixels as nodes. Using affinity matrices, the nodes are ranked according to the similarity to background and foreground queries. In [31] a measure to estimate how heavily a region is connected to the image borders is adopted. Then, a principled optimization framework to incorporate multiple low-level cues, including the background measure, is employed to obtain clean and uniform saliency maps. The method in [32] is based on the computation of global contrast difference and of spatially weighted coherence scores. The detection of salient regions is obtained by using the saliency maps to initialize a new iterative version of GrabCut [50].

The application of saliency-based methods to dermoscopy is relatively new [17, 33-34]. Saliency-based lesion skin segmentation methods compute the salient region in an image according to human visual perception such that a salient (not salient) region becomes foreground (background) region, namely skin lesion (healthy lesion). In [17] saliency combined with Otsu threshold is proposed for the automatic skin lesion segmentation. The method includes two phases: enhancement and segmentation. In the first phase (enhancement), the color saliency map and brightness saliency map are computed and fused to obtain the final enhanced image. In the second phase (segmentation), to obtain more accurate lesion borders, an optimization function is designed to adjust the traditional Otsu threshold method according to the histogram distribution of the enhanced image. In [33] the saliency is computed by using the reconstruction errors derived from a sparse representation model and a novel background detection process. The shape and the borders of the lesion are delineated in a Bayesian framework. In [34], the contrast of the skin lesion and healthy skin is increased by the fusion of the corresponding saliency maps. Then, an adaptive wavelet-based thresholding method is employed.

However, saliency is not the only useful feature to handle the skin lesion segmentation task. Indeed, color is one of the most cues that humans use extensively to detect an object.

Especially, color is widely used to detect lesion by dermatologists since, as said above, to accurately detect the skin lesion it is extremely important to amount the color of melanin which depends on its localization in the different layers of the skin [1]. Indeed, color information is widely used in medical image analysis and also in skin lesion segmentation [51-53]. Color information has been also used in saliency-based methods not designing for skin lesion segmentation [37-39], while in saliency-based lesion segmentation the use of color information results be of limited use. In particular, a perceptual color difference saliency with morphological analysis has been recently proposed [40].

Therefore, the rationale for integrating the saliency with color information, which is the main aim of the present paper, is that their combined use can significantly improve the segmentation results in presence of low contrast and can permit to face the critical issues, typically not resolved by many of the existing saliency-based segmentation methods, which occur in correspondence of salient regions sharing similar color features with the background.

3. The proposed method

As mentioned in the introduction and section 2, the objective of the proposed segmentation method, SCS, is to segment dark skin lesions in dermoscopic images using two different types of information: saliency and color.

Skin lesion segmentation task has a complex nature due to some problems such: (a) the presence of artifacts with various nature; (b) the presence of hair on the skin; (c) the existence of different colors within the lesion; (d) the low contrast at the border separating the lesion from the surrounding healthy skin. In particular, some artifacts, e.g., dark corners, ink markers, rulers, and bubbles, are caused directly by the imaging technique. The presence of hair (also considered as artifacts) and/or different colors inside the lesion are due to the nature of the image, while the low contrast is usually due to different conditions of illumination, contrast, and noise. In Figure 1, some examples are shown. Since the presence of artifacts as well as of aberrations greatly affects the accuracy of the segmentation, the most of the skin lesion segmentation methods are designed so that all artifacts and effects of bad illumination are removed, or at least mitigated, before applying the segmentation process which should be able to treat adequately the remaining undesired effects.

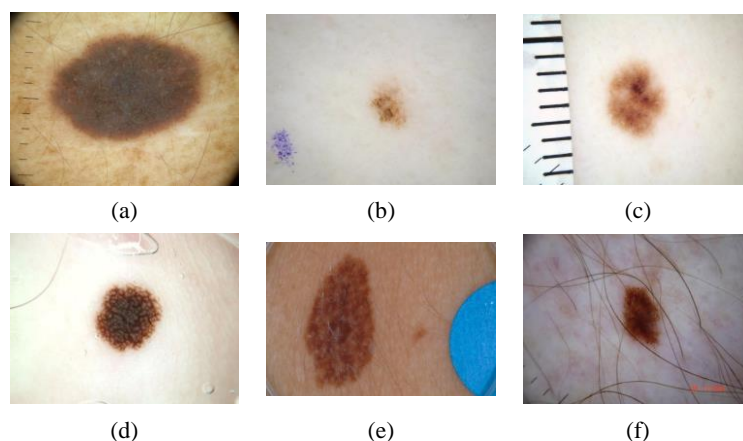


Figure 1. Examples of possible artifacts and aberrations.

The method SCS follows this algorithmic scheme. It consists of two consecutive main steps: pre-processing and segmentation. The pre-processing step is aimed mainly at preparing the image for eliminating artifacts (a) and hair (b) and to compute the Saliency Map (SM). The core step is the successive segmentation which determines, in terms of visual appearance (saliency) and color, a Binary Mask (BM) representing the localization of the skin lesion which is then employed to determine the skin lesion. This innovative step allows overcoming in most cases the problems due to different colors (c) and low contrast (d). In the flowchart of Figure 2, the proposed method is schematically shown.

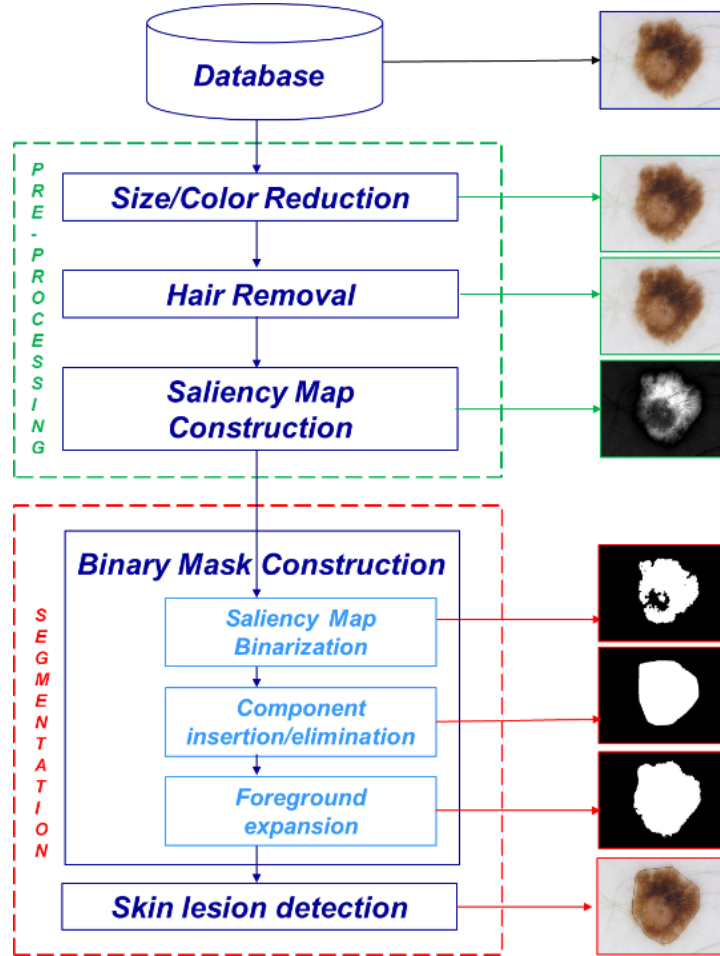


Figure 2. Flowchart of the proposed method, SCS.

3.1. Pre-processing step

The pre-processing step consists of three sub-steps. The first sub-step, namely Size/Color Reduction (A.1), is devoted to limit the computation burden of the successive steps by reducing the size and number of colors. This early sub-step is an optional but highly recommended operation since it significantly limits the computation time. The target of the second sub-step, namely Hair Removal (A.2), is to remove or, at least to limit, the sign of hair since the resulting segmentation could be influenced by it. The third sub-step, namely Saliency Map Construction (A.3), is for the computation of the saliency which is one of the two main information considered as useful for skin lesion detection. In more detail, the pre-processing step can be outlined as follows.

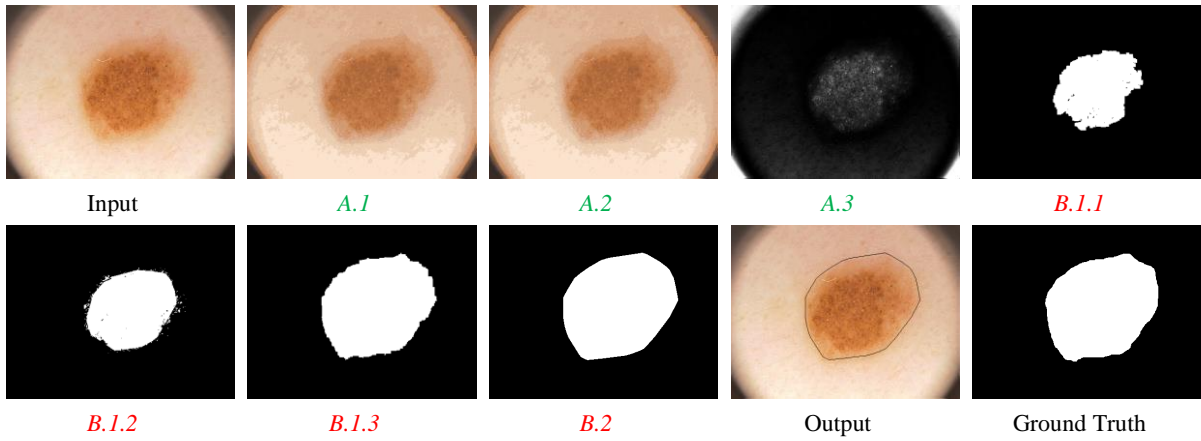


Figure 3. Results of each step by SCS on an image of PH² database and the corresponding ground truth.

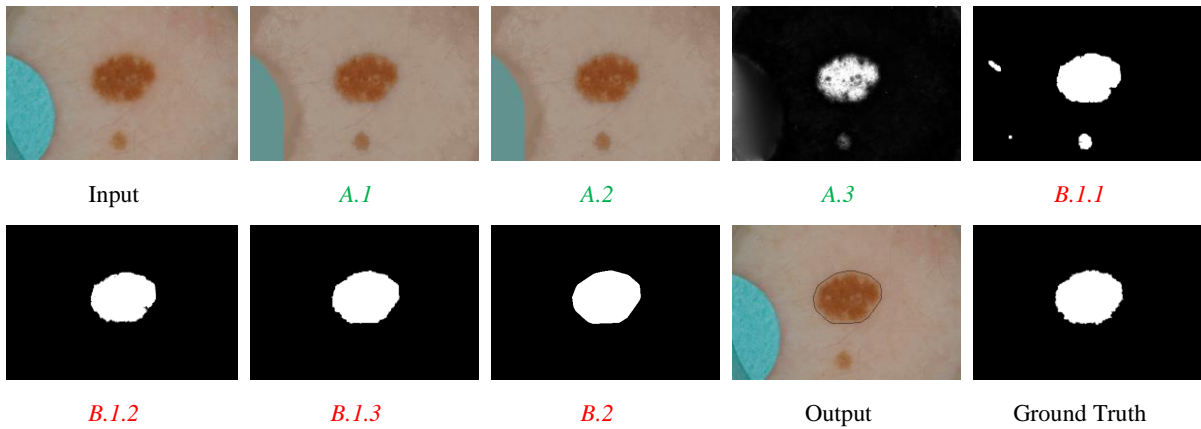


Figure 4. Results of each step by SCS on an image of ISIC2016 database and the corresponding ground truth.

A.1 - Size/Color Reduction. The size of the image is reduced so that the maximum between the number of rows and the number of columns is equal to a value fixed by the user, say *Maxdim*. Downsampling is done using bicubic interpolation. The reduction of the number of colors is obtained by a Color Quantization (CQ) method. Four different CQ methods are available to this purpose: [13, 41–43]. The number of colors, namely *colnum*, is fixed by the user.

A.2 - Hair Removal. Since the presence of hair, which typically appears superimposed and/or close to the lesion, can lead to not suitable segmentation, e.g. see the example shown in Figure 1f), the hair present in the lesion image is removed and the position of the image in correspondence with the removed hair is restored by the algorithm in [21]. Unfortunately, hair removal is not always completely successful. The influence of hair not perfectly removed and of other artifacts is strongly reduced in the following steps by suitable operations based on saliency and color information.

A.3 - Saliency Map Construction. SM with well-defined boundaries of salient objects is computed by the method proposed in [37] or in [38]. The Saliency Map is then enhanced by increasing the contrast in the following way: the values of the input intensity image are mapped to new values obtained by saturating the bottom 1% and the top 1% of all pixel values.

3.2. Segmentation step

The segmentation step consists of two main sub-steps: Binary Mask Construction (B.1) and Skin Lesion Detection (B.2). The first sub-step (B.1) detects the Binary Mask delimiting the region of interest, then used to determine the skin lesion (B.2).

B.1 - Binary Mask Construction. To compute the Binary Mask three main sub-steps are required: Saliency Map Binarization (B.1.1), Component inclusion/elimination (B.1.2), Foreground Expansion (B.1.3). The first sub-step (B.1.1) extracts the more salient regions and detects the initial Binary Mask. The second (B.1.2) and the third sub-steps (B.1.3) are devoted respectively: i) to eliminate false salient regions due to bad illumination or due to low contrast; ii) to insert/eliminate regions in the binary mask by considering saliency and color information. In more detail, the step of Binary Mask Construction can be described as follows.

B.1.1 - Saliency Map Binarization. The strategy initially adopted in this step is to identify the “core” of the lesion, the initial Binary Mask, by an iterated process based on saliency information. Thus, SM undergoes an iterated binarization process aimed at extracting the more salient regions. At each iteration, SM is binarized in the following way. All pixels with saliency value greater than the average saliency value μ_s are recorded into a Binary Mask (BM), initially empty, and considered as belonging to the foreground of BM, shortly indicated as BM-foreground (BM_f), while all other pixels are assigned to background of BM, shortly indicated as BM-background (BM_b).

Let R_f (R_b) be respectively the connected components of BM_f (BM_b), the average saliency value μ_s is newly computed by ignoring the pixels belonging to connected components R_f which include pixels on the image frame. Generally, a smaller average saliency value μ_s is obtained so that, when the SM is newly binarized for the computed new saliency value, a larger number of pixels overcome this new threshold value, which is selected as potentially belonging to BM_f . The process for saliency map binarization is iterated as far as connected components including pixels of the image frame are detected. BM constitutes the initial Binary Mask.

Note that this iterated process is necessary to manage some images where the average saliency value is strongly conditioned by the presence of artifacts caused directly by the adopted image acquisition technique. This is the case, for example, when are present dark corners, see Figure 1a), or, even worse, when the region of interest for saliency map thresholding constitutes a circular portion of an otherwise completely dark image. In the presence of these dark artifacts, which are characterized by a rather high saliency value, the average saliency value would be higher than the average saliency value characterizing the pixels in the skin lesion. As a consequence, the number of pixels that would be assigned to BM_f is remarkably smaller than expected. For this reason, saliency map binarization involves a process aimed at identifying a Binary Mask including all pixels whose saliency value should not be counted for average saliency value computation. Moreover, an iterated process is performed to identify BM since not all pixels of the artifacts are characterized by the same (high) saliency value.

Successively, as mentioned in section 2, since saliency information alone might not be enough to characterize the lesion, and at the same time, color information is one of the key

factors for skin lesion detection [1, 11-14], to identify the lesion in addition to saliency-based criteria, we introduce some criteria, inspired by human visual perception and related to color and saliency information. Accordingly, in the successive steps *B.1.2* and *B.1.3*, connected components (regions) are eventually aggregated to BM or eliminated based on color information and the visual context.

B.1.2 - Component insertion/elimination. A critical configuration for the construction of BM can occur when the BM_b , normally lighter than the BM_f , includes some regions that are lighter than the remaining background regions. Indeed, since salient regions are regions visually more evident than the surrounding areas, it may happen that both pixels inside the lesion, hence characterized by darker colors, and pixels in the lightest portions of the BM_b have high enough saliency that makes them potentially assignable to BM_f during binarization. The solution to this problem is obtained by introducing *the property of color proximity* and by resorting to the *color proximity criterion* (1) defined as follows.

Color proximity property: the lesion can also include regions with not high saliency but having average color “perceptually close” to the color of the skin lesion already detected.

More specifically:

C^* : the darkest detected color of BM_f ,

C_f : the average color associated to each R_f of BM_f , for $f=1, \dots, N$

$d_f(C_f, C^*)$: the distance of the average color C_f from C^* , for $f=1, \dots, N$

$d_{\min} = \min\{d_f(C_f, C^*)\}$, for $f=1, \dots, N$

$d_{\max} = \max\{d_f(C_f, C^*)\}$, for $f=1, \dots, N$

$\Delta = d_{\max} - d_{\min}$

$\delta = \text{mean}(d_{\max}, d_{\min})$

we postulate that “a small value of Δ implies that the BM_f includes connected components characterized by average colors perceptually close that should be maintained in the BM_f , while a large Δ implies that the components are characterized by rather different average colors”. As a consequence, some of these components should be disregarded and not considered as belonging to the lesion.

According to this *color-proximity property*, we adopt the following *color proximity criterion*.

Color proximity criterion: if Δ is greater than a threshold value T_c than remove from BM_f the components R_f characterized by an average color C_f larger than δ :

$$\text{if } \Delta > T_c \ \& \ (\exists R_f \in BM_f : C_f > \delta) \Rightarrow (R_f \notin BM_f) \ \& \ (R_f \in BM_b) \quad (1)$$

where T_c is a prefixed threshold value on the color difference perceptible to the human eye.

As follows, we accept as belonging to BM_f also some pixels characterized by low saliency values that prevented their extraction during binarization, provided that their colors are closer to the average color of BM_f than to the average color of the BM_b .

Currently, BM is likely to consist of some components, all characterized by saliency or color compatible with those expected for the skin lesion to be segmented. However, not all

these components do belong to the skin lesion. Some peripheral parts can be just noisy regions characterized by saliency or color very similar to those in the skin lesion. To keep only the relevant components, we distinguish the remaining R_f in kernel and peripheral component according the following definition of *peripheral* and *kernel component*.

Peripheral/kernel component definition: a component R_f including less of T_n pixels with saliency greater than $2\mu_s$ is considered as peripheral component” (i.e. belonging to the set PC of the peripheral components of BM_f) otherwise it is a kernel component, (i.e. belonging to the set KC of the kernel components of BM_f).

Moreover, denoting:

$CH(KC, R_f)$: the convex hull of KC plus the peripheral component R_f

$CH(KC)$: the convex hull of the kernel components KC

$A[KC]$: the total area of the kernel components KC

$A[R_f]$: the area of the R_f component

$A[CH(KC, R_f)]$: the area of $CH(KC, R_f)$

$A[CH(KC)]$: the area of $CH(KC)$

$AD = A[CH(KC, R_f)] - A[CH(KC)] - A[R_f]$

rig: number of rows of the input image

col: number of rows of the input image

$minsize = \min(rig, col)$;

we estimate the proximity of a peripheral component R_f to the kernel KC according to the following *kernel proximity property*.

Kernel proximity property: R_f is sufficiently close to KC if $A[R_f]$ is less than AD, i.e. AD is sufficiently small”.

Then, to ascribe eventually the peripheral components to BM_b , based on the *peripheral/kernel component* definition and the *proximity kernel proximity*, we apply the following criterion, namely *peripheral component criterion* (2).

Peripheral component criterion: if a peripheral component R_f has area $A[R_f]$ less than of a significant percentage, namely θ_l , of minsize or larger than $A[KC]$ or R_f is sufficiently close to KC, (i.e. $A[R_f] < AD$) then ascribe it to BM_b :

$$\text{if } (A[R_f] < \theta_l \cdot minsize \parallel A[R_f] > A[KC] \parallel A[R_f] < AD) \Rightarrow (R_f \notin BM_f) \& (R_f \in BM_b) \quad (2)$$

An example is shown in Figure 3-4, step B.1.2.

B.1.3 - Foreground expansion. In many cases, the segmented BM_f obtained at the end of the previous step is already close enough to the desired result. However, there are skin lesions for which the color transition from foreground to background is not sharp. In these cases, a sort of band, namely *Color Transition Region (CTR_f)*, surrounding the detected foreground can be noted in SM. To detect lesion components in correspondence of the region surrounding the detected BM_f , in which the color transition from lesion foreground to background is not sharp, color information and the property of *color proximity* are also employed.

In particular, the surrounding region CTR_f is detected by considering from saliency map

SM pixels not belonging to BM_f , having low saliency values, say smaller than a prefixed value, namely T_s , but having rather different colors according to the above property of *color proximity*. Thus, indicated by:

- C_m : the average color of the current CRT_f
- C_b : the average color of CRT_b
- $d(C_b, C_m)$: the distance of the average color C_b from C_m
- C_p : the color of a pixel $p \in CRT_f$
- $dp(C_p, C_m)$: the distance of the average color C_p from C_m

we filter out from CRT_f the pixels that cannot be assigned to CRT_f , that is any pixel p of CRT_f whose color C_p has distance from C_m larger than a significant percentage, namely θ_2 , of $d(C_b, C_m)$ is assigned to CRT_b :

$$\forall p \in CRT_f: dp(C_p, C_m) > \theta_2 \cdot d(C_b, C_m) \Rightarrow (p \notin CRT_f) \ \& \ (p \in CRT_b) \quad (3)$$

Then, the remaining pixels of CRT_f not belonging to BM_f but connected to BM_f are assigned to BM_f according to (4)

$$\forall p \in CRT_f, p \notin BM_f, p \text{ connected to } BM_f \Rightarrow p \in BM_f \quad (4)$$

As an example, see Figure 3-4, step B.1.3.

B.2 - Skin Lesion Detection. This step refines the obtained BM to better select the lesion regions among the possible candidates to improve the final shape and to make it better compliant to the region manually delineated by the skin specialist. To this purpose, morphological operations are applied to smooth the contour of the segmented skin lesion and fill possibly existing small holes.

If more than one component is obtained, since for the considered databases (ISIC2016 and PH²) only one lesion component is expected, the one with the largest area is selected. The convex hull of such a component is finally computed. It constitutes the result of segmentation. In the alternative, in case of the considered database foresees more than one possible lesion, this step is skipped.

In Figure 3 and Figure 4, the results obtained in each step by SCS are shown for an image of PH² and ISIC2016, respectively. In Figure 5, a few examples of the results under varying critical conditions (see Figure 1), such as the presence of a dark halo, blue ink stains, a ruler, air bubbles, colored disks, thick hair, are shown. Other results with different performances are shown in Figure 6. For each example in Figure 5-6, the quality performance evaluation metrics, mentioned and defined respectively in section 4 and Table 1, are given. In Figure 6, a comparison of the segmentation result with the ground truth, see the ultimate column, is also visualized where white is used for True Positive (TP) pixels, red for False Positive (FP), and green for False Negative (FN) pixels. In Figure 3-6 the detected boundary of the segmented skin lesion is shown superimposed onto the input.

Note that: a) while the reduction of noise on the contour as well as the elimination of isolated and small regions helps to improve the skin lesion detection, the selection of the lesion region in case more than one has been detected is a necessary step for the databases under consideration. b) the convex hull is computed since, especially for ISIC2016 images, even when the skin contour is visually well delineated, in most cases the contour provided by

convex hull usually better adapts to the skin border of ground truth [54]. See the examples in Figure 3-6. c) the segmentation step requires to establish the values of five perceptive threshold values: T_c (relative to the color difference perceptible to the human eye), T_n (relative to the minimum number of pixels with high saliency of a peripheral component), θ_1 (relative to the percent of the minimal area visible to the human eye), T_s (relative to the saliency values considerable as not salient), θ_2 (relative to the percent on color distance perceptible to the human eye). The choice of the value of these parameters depends on the class of images to handle. Their values have been experimentally determined for the database PH² and ISIC2016 (see subsection 4.2).

4. Performance evaluation

4.1. Databases

We have tested our method on two publicly available databases of dermoscopic images: PH2 [44] and ISIC2016 [45].

PH² is a dermoscopic image database acquired at the Dermatology Service of Hospital Pedro Hispano to support comparative studies on segmentation/classification methods. This database includes clinical/histological diagnosis, medical annotation, and the evaluation of many dermoscopic criteria. It provides 200 dermoscopic RGB images and the corresponding ground truth, including 80 atypical nevi, 80 common nevi, and 40 melanomas. All the images are 8-bit RGB and have resolution 760x560 pixels.

ISIC2016 is one of the largest databases of dermoscopic images of skin lesions with quality-controlled held by the International Symposium on Biomedical Imaging (ISBI) to improve melanoma diagnosis. It includes images representative of both benign and malignant skin lesions. For each image, the ground truth is also available. Parts of the ISIC2016 dataset that we have used in this paper consist of 397 (75 melanomas) and 900 (173 melanomas) annotated images for testing and training, respectively. The images are 8-bit RGB and have a size ranging from 542x718 to 2848x4288.

PH² and ISIC2016 datasets contain numerous images with complex background and complicated skin conditions with the presence of various artifacts and aberrations. We point out that not all ground truth images are characterized by the same high level of detail. Indeed, mainly in ISIC2016, in some ground truth images, the lesion's boundary is delineated very accurately, which is typical of results obtained by an automatic segmentation software, while for other images the boundary is more roughly approximated, which is typical of segmentation manually achieved by the dermatologists.

4.2. Qualitative evaluation

The segmentation results obtained by SCS have been qualitatively analyzed and compared with the results obtained by existing saliency-based segmentation methods [17, 30-34] using the images available in PH2 and ISIC2016 databases. For most of the examined images, as can be seen by the examples shown in Figure 3-6, the skin lesions are correctly detected by SCS with well-defined boundaries. For the images including hair and characterized by similar colors in the region of the skin lesion and of the background, this is also evident. Moreover, it can be observed that the proposed method accomplishes appropriate results for

images having high contrast, see for instance Figure 6.

As the employed datasets consist of images of different sizes, we have selected the minimum common dimension setting $maxdim=500$. As well, given the different number of colors for the available images, a good compromise has been to set $colnum=64$. To determine the best perceptual parameter values, we manually minimized over the whole PH² dataset the resulting metrics values. Then, we validated those values on the ISIC2016 dataset. Since the SCS performance is slightly better when CQ and Saliency Map are computed respectively by [38] and [41] and when we set the following parameters: $T_c=60$, $T_n=50$, $\theta_l=0.2$, $T_s=10$, $\theta_2=0.8$, in the overall paper, the examples and the Tables are relative to the above-selected methods and setting.

However, SCS may fail to identify accurately the skin lesion when the pre-processing phase has not been sufficient to clean properly the image. For instance, when the hair has been only partially removed in sub-step A.2. Moreover, for a limited number of cases the non-correct obtained result is intrinsically explained by the fact that we rely segmentation on saliency while, for some images, saliency is not adequate to extract the desired foreground. For instance, when the highest saliency values are found in the background while saliency value within the skin lesion is extremely low. Finally, the aforementioned different high level of detail of the ground truth justifies the fact that our results are sometimes very close to the ground truth images, while sometimes differ more from those.

Table 1. Evaluation Metrics, where FP, FN, TP and TN respectively denote False Positive, False Negative, True Positive and True Negative assessments.

Symbol	Metric	Definition
AC	Pixel-level accuracy	$AC = \frac{TP + TN}{TP + FP + TN + FN}$
SE	Sensitivity	$SE = \frac{TP}{TP + FN}$
SP	Specificity	$SP = \frac{TN}{TN + FP}$
DI	Dice coefficient	$DI = \frac{2 * TP}{2 * TP + FN + FP}$
JA	Jaccard index	$JA = \frac{TP}{TP + FN + FP}$
P	Precision	$P = \frac{TP}{TP + FP}$
E	Error	$E = \frac{FP + FN}{TP + FP + TN + FN}$
HD	Hamoude distance	$HD = \frac{FP + FN}{TP + FN + FP}$
XOR	XOR	$XOR = \frac{FP + FN}{TP + FN}$

4.3. Quantitative evaluation

The segmentation results obtained by SCS have been quantitatively evaluated using the images available in PH2 and ISIC2016 databases [44,45], comprising in total 1497 images.

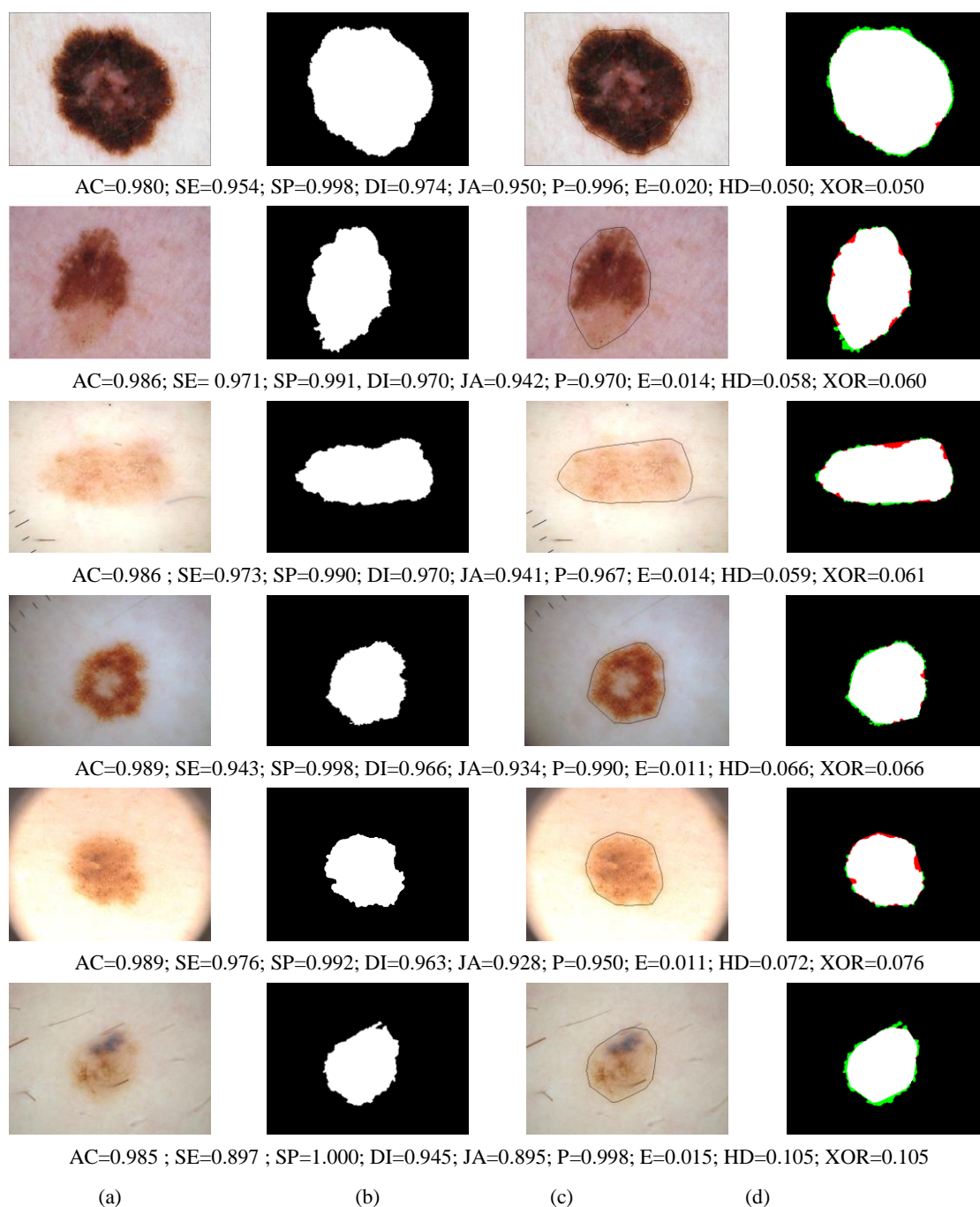


Figure 5. a) Inputs; b) ground truths; c) different performance of SCS on images of the two databases, where detected boundary is shown superimposed onto the input; d) comparison of the segmentation results with the ground truth, where white is used for TP, red for FP and green for FN pixels.

On these databases, we have compared the performance of SCS with that of classical saliency-based methods including MR [30], RBD [31], RC [32] and with that of some more recent saliency-based methods specifically applied to dermoscopic images including Fan [17], RSSLS [33], Hu [34] in terms of the following evaluation metrics: Pixel-level accuracy (AC), Sensitivity or Recall (SE), and Specificity (SP), Dice coefficient or F-measure (DI) and Jaccard index (JA) as well as Precision (P), Error (E), Hamoude distance (HD) and XOR (XOR) as defined in [34, 55] and reported in Table 1.

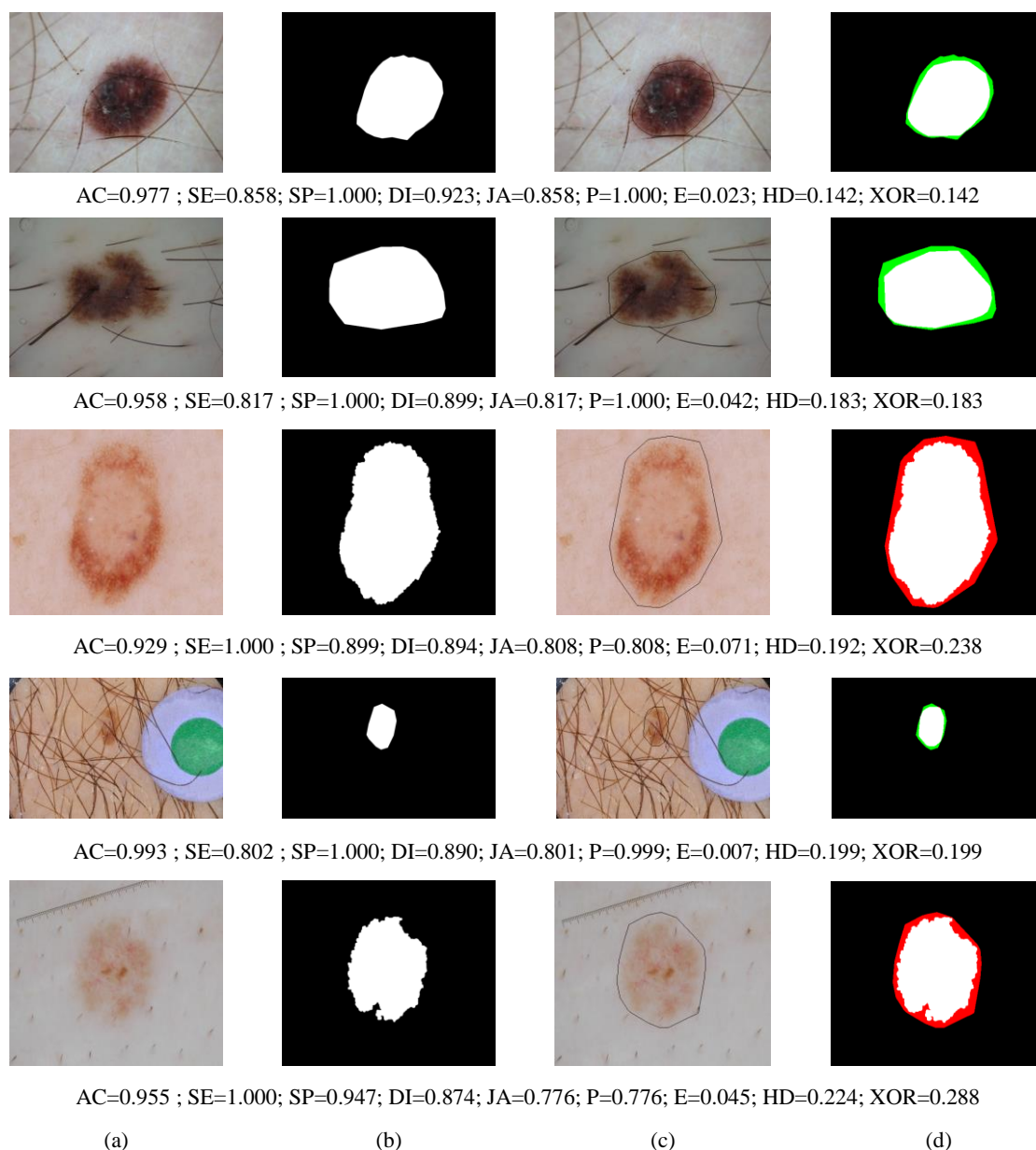


Figure 5 (continued).

We remark that for the quantitative comparison, we select [17, 30-34] among the existing saliency-methods because they show results on the full databases under examination [44, 45] and use most of the metrics we adopted. Unfortunately, it is not possible to compare the results obtained by [40] since the implementation of the method is not available and the published results refer to only 120 unspecified images belonging to the two databases [44, 45].

The validation of the proposed method has been done by applying different methods for saliency detection [37-38] and CQ [13, 41-43] as well as by using a different choice of the parameters. This validation has highlighted that SCS essentially is independent of the selection of the employed methods and parameters since it shows comparable and consistent performance with the other choices regarding CQ and saliency detection procedure. In this paper, the examples and the Tables referred to SCS performance are obtained using the methods [38, 41] and setting the perceptive thresholds to the values indicated at the end of

section 3.

The average of the evaluation metrics of the considered benchmark methods and SCS for PH² and ISIC2016 are shown in Table 2 and Table 3 and Table 4, respectively. The performance evaluation values regarding the benchmark methods have been taken from the cited papers [17, 30-34] and [44]. This comparison is limited to 1100 images since the average of the evaluation metrics are available only for PH² and the Train Set of ISIC2016. In Table 4, the average of the evaluation metrics of the considered benchmark methods and SCS for the Test Set is shown. The distribution of the average values of the quality measures (DI, HD, XOR) employed in almost all benchmarking methods is shown in Figure 7.

Note that resulting quality values for PH² in Table 2 could be improved if the convex hull is not computed in the final step since, differently from ISIC2016, the lesion's boundary of the ground truth is accurately detected. However, to compare with the results obtained on ISIC2016 images, the computation of the convex hull is performed also for PH² images.

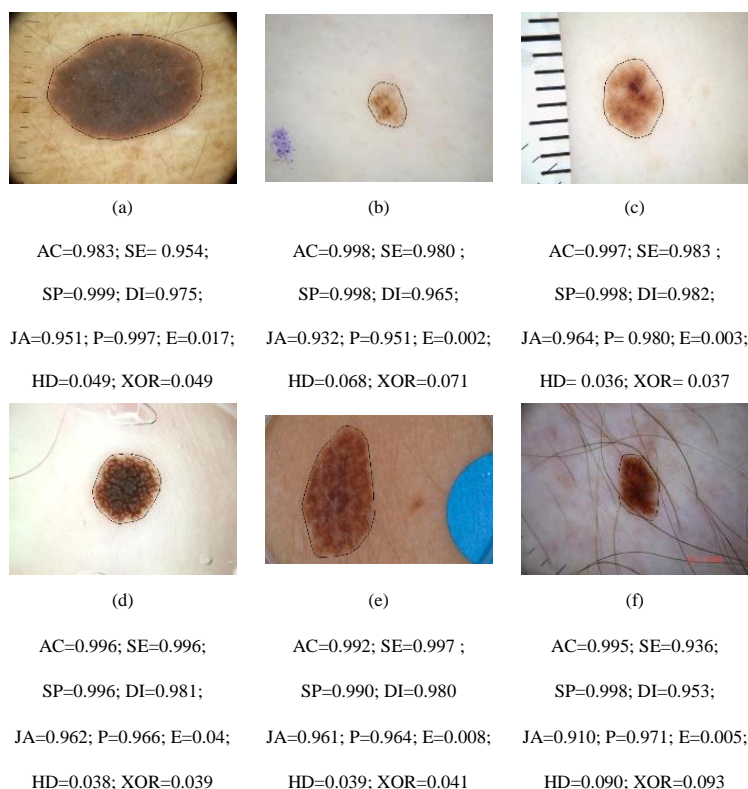


Figure 6. Results by SCS on the image examples with artifacts and/or aberrations shown in Figure 1.

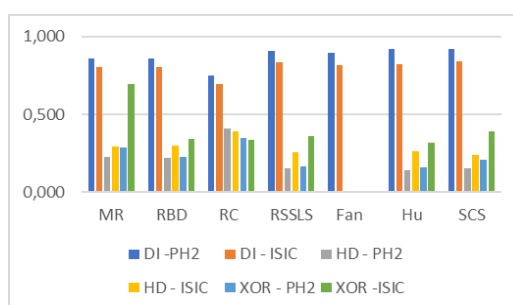


Figure 7. Average quality values of benchmark methods (MR, RBD, RC, RSSLS, Fan, Hu) and SCS using PH² and ISIC2016 databases.

5. Discussion and conclusions

In this paper, we propose the method SCS which, being based on saliency, can be ascribed to the exiting class of saliency-based methods although it should be classified as belonging to a wider class since, to the best of our knowledge, the proposed paper is among the first to employ saliency and color information simultaneously which is considered by a dermatologist as essential to performance lesion detection. SCS, based on the combined use of saliency and color turns out a robust, appropriate, and flexible method with better performance respect to only saliency-based methods.

The proposed method is an extension of the preliminary version to segment skin lesions in dermoscopic images [14] and consists of two consecutive main steps: pre-processing and segmentation.

The first step is devoted to image preparation. Initially, the computation burden of the segmentation process is optionally lowered by reducing the size of the images as well as the number of colors. Then, the image undergoes a hair removal process, after which the saliency map is computed and the contrast of the map is increased. We note that since the presence of hair could strongly have a bad influence on the skin lesion region detection in the successive step, the selection of a better hair removal algorithm could facilitate further the obtained segmentation results.

The second step is devoted to the construction of the Binary Mask including the skin lesion. Through an iterated process, an initial Binary Mask is built so that to exclude artifacts such as dark corners and to work only on the portion of the image which includes the lesion and the surrounding skin. Successively, components not ascribed to the Binary Mask, due to their saliency level that is lower than the threshold, but with noticeable color information and not sharp color transition from foreground to background, are possibly assigned to the Binary Mask. Finally, morphological operations are applied to improve the shape of the Binary Mask foreground, the component with a maximal area is selected and its convex hull is taken as the segmentation result. This second step (segmentation) is completely new and constitutes the main contribution of the paper since it is based on the new properties/criteria related to color and saliency information which are suitably employed according to the context. The segmentation process is flexible since new properties and criteria can be added eventually considering other types of information besides saliency and color.

SCS is independent of the adopted computation methods employed in the first step. To give evidence to this aspect we use the proposed method as a baseline to employ different methods for color quantization and saliency computation and to test the effects of this preliminary processing. The performance of the proposed method and eventual dependencies from color and saliency computation has been extensively evaluated by considering two publicly available databases. This evaluation is mainly based on the qualitative comparison of results to the ground truth provided in the database, and quantitatively in terms of nine commonly adopted quality measures. Finally, a different parameter setting to achieve a trade-off between quality and performance has been explored.

Based on the performance evaluation and of the obtained quality values, SCS achieves good quantitative results with an adequate balance. Overall, SCS has a competitive and satisfactory performance concerning other existing saliency-based methods as the probability

of missing salient regions and/or the detection of falsely marked salient background regions is low. Moreover, it detects rapidly salient regions having limited complexity. The results have also demonstrated the effectiveness and the utility of the employment of saliency and color information for skin lesion segmentation. Finally, the implementation does not require any extensive learning based on a very large number of parameters and of labeled training images and its execution time is rather fast.

Table 2 – Results of PH² dataset segmentation (200 images).

Method	AC	SE	SP	DI	JA	P	E	HD	XOR
MR [30]	-	-	-	0.861	-	-	-	0.226	0.288
RDB [31]	-	-	-	0.862	-	-	-	0.219	0.228
RC [32]	-	-	-	0.748	-	-	-	0.410	0.350
RSSLS [33]	-	-	-	0.910	0.682	-	-	0.155	0.165
Fan [17]	-	0.870	-	0.893	-	0.968	0.064	-	-
HU [34]	-	0.942	-	0.922	-	0.913	0.053	0.139	0.159
SCS	0.954	0.952	0.955	0.921	0.900	0.921	0.076	0.155	0.205

Table 3 – Results of ISIC2016 Train Set segmentation (900 images).

Method	AC	SE	SP	DI	JA	P	E	HD	XOR
MR [30]	-	-	-	0.807	-	-	-	0.295	0.693
RDB [31]	-	-	-	0.804	-	-	-	0.300	0.341
RC [32]	-	-	-	0.697	-	-	-	0.393	0.338
RSSLS [33]	-	-	-	0.834	-	-	-	0.257	0.362
Fan [17]	-	0.747	-	0.818	-	0.973	0.082	-	-
HU [34]	-	0.766	-	0.824	-	0.964	0.081	0.262	0.314
SCS	0.910	0.832	0.958	0.843	0.860	0.961	0.098	0.239	0.390

Table 4 – Results of ISIC2016 Test Set segmentation (379 images).

Method	AC	SE	SP	DI	JA	P	E	HD	XOR
SCS	0.962	0.899	0.975	0.877	0.891	0.921	0.045	0.159	0.303

Acknowledgments

This work has been supported by GNCS (Gruppo Nazionale di Calcolo Scientifico) of the INDAM (Istituto Nazionale di Alta Matematica).

References

1. H.P. Soyer, G. Argenziano, I. Zalaudek, R. Corona, F. Sera, R. Talamini, F. Barbato, A. Baroni, L. Cicale, A. Di Stefani, P. Farro, L. Rossiello, E. Ruocco, S. Chimenti, “Three-point checklist of dermoscopy. A new screening method for early detection of melanoma,” *Dermatology*, vol. 208, pp. 27–31, 2004.
2. A. Perrinaud, O. Gaide, L.E. French, J.H. Saurat, A.A. Marghoob, R.P. Braun, “Can automated dermoscopy image analysis instruments provide added benefit for the dermatologist? A study comparing the results of three systems,” *Br. J. Dermatol.*, vol. 157, pp. 926–933, 2007.
3. S.W. Menzies, L. Bischof, H. Talbot et al., “The performance of SolarScan: an automated dermoscopy image analysis instrument for the diagnosis of primary melanoma,” *Archives of Dermatology*, vol. 141, no. 11, pp. 1388–1396, 2005.
4. M. Binder, M. Schwarz, A. Winkler et al., “Epiluminescence microscopy: a useful tool for the diagnosis of pigmented skin lesions for formally trained dermatologists,” *Archives of Dermatology*, vol. 131, no. 3, pp. 286–291, 1995.

5. G. Zouridakis, M.D.M. Duvic, N.A. Mullani, "Transillumination imaging for early skin cancer detection," Tech. Rep. Biomedical Imaging Lab, Department of Computer Science, University of Houston, Houston, Tex, USA, 2005.
6. N.K. Mishra, M.E. Celebi, "An Overview of Melanoma Detection in Dermoscopy Images Using Image Processing and Machine Learning," arXiv:1601.07843 [cs.CV], 2016.
7. E. Okur, M. Turkan, M., "A survey on automated melanoma detection," *Eng. Applications of Artificial Intelligence*, vol. 73, pp. 50-67, 2018.
8. R.B. Oliveira, J.P. Papa, A.S. Pereira, J.M.R.S Tavares, "Computational methods for pigmented skin lesion classification in images: review and future trends", *Neural Comput. & Applic.*, vol. 29, pp. 613-636, 2018.
9. J. Premaladha, M. Lakshmi Priya, S. Sujitha, K. S. Ravichandran, "A Survey on Color Image Segmentation Techniques for Melanoma Diagnosis", *Indian J Science and Technology*, vol. 8, no. 22, IPL0265, 2015.
10. M.J. Scott Henning, S.W. Dusz, S. Q. Wang, A.A. Marghoob, H.S. Rabinovitz, D. Polsky, A.W. Kopf, "The CASH (color, architecture, symmetry, and homogeneity) algorithm for dermoscopy", *J. Am. Acad. Dermatol.*, vol. 56, pp. 45–52, 2007.
11. G. Ramella, G. Sanniti di Baja, "Image segmentation based on representative colors and region merging," in *Pattern Recognition*, J. A. Carrasco-Ochoa et al Eds., Lecture Notes in Computer Science 7914, Springer, 2013, pp. 175-184.
12. G. Ramella, G. Sanniti di Baja, "From color quantization to image segmentation," in *Proc. 12th Int. Conf. on Signal Image Technology & Internet-Based Systems - SITIS 2016*, K. Yetongnon et al. Eds., IEEE Computer Society, 2016, pp. 798-804.
13. V. Bruni, G. Ramella, D. Vitulano, "Perceptual-based Color Quantization," in *Image Analysis and Processing - ICIAP 2017*, S. Battiato et al. Eds., Lecture Notes in Computer Science 10484, Springer, 2017, pp. 671 - 681.
14. G. Ramella, "Automatic Skin Lesion Segmentation based on Saliency and Color," in *VISAPP 2020*, G. M. Farinella et al. Eds., Scitepress Science and Technology Publications, vol. 4, 2020, pp. 452-459.
15. K.N. Plataniotis, A.N. Venetsanopoulos, *Color Image Processing and Applications*, Springer Science & Business Media, 2013.
16. M. E. Celebi, G. Schaefer (eds.), *Color Medical Image Analysis*, Lecture Notes in Computational Vision and Biomechanics, vol. 6, 2013.
17. H. Fan, F. Xie, Y. Li, Z. Jiang, J. Liu, "Automatic segmentation of dermoscopy images using saliency combined with Otsu threshold," *Comput Biol Med.*, vol. 85, pp. 75–85, 2017.
18. J. Quintana, R. Garcia, L. Neumann, "A novel method for color correction in epiluminescence microscopy", *Comput. Med. Image Graph.*, vol. 35, no. 7, pp. 646–652, 2011
19. J. Glaister, R. Amelard, A. Wong, D. Clausi, "MSIM: multistage illumination modeling of dermatological photographs for illumination-corrected skin lesion analysis," *IEEE Trans Biomed Eng.*, vol. 60, no. 7, pp. 1873–1883, 2013.
20. C. Barata, M.E. Celebi, J.S. Marques, "Improving dermoscopy image classification using color constancy," *IEEE J Biomed Health Inform.*, vol. 19, no. 3, pp. 1146–1152, 2015.
21. T. Lee, V. Ng, R. Gallagher, A. Coldman, D. McLean, "Dullrazor: A software approach to hair removal from images," *Comput. Biol. Med.*, vol. 27, no. 6, pp. 533–543, 1997.
22. M. Silveira, J. C. Nascimento, J. S. Marques, A. R. Marçal, T. Mendonça, S. Yamauchi, J. Maeda, J. Rozeira, "Comparison of segmentation methods for

- melanoma diagnosis in dermoscopy images," *IEEE Journal of Selected Topics in Signal Processing*, vol. 3, no. 1, pp. 35–45, 2009.
23. K. Korotkov, R. Garcia, "Computerized analysis of pigmented skin lesions: A review," *Artificial Intelligence in Medicine*, vol. 56, pp. 69–90, 2012.
 24. A. Masood, A. A. Al-Jumaily, "Computer Aided Diagnostic Support System for Skin Cancer: A Review of Techniques and Algorithms," *Int. J. Biom. Imag.*, Hindawi Publishing Corporation, Article ID 323268, 22 pages, 2013.
 25. H. Zhou, X. Li, G. Schaefer, M.E. Celebi, P. Miller, "Mean shift based gradient vector flow for image segmentation," *Comput. Vis. Image Understanding*, vol. 117, pp. 1004–1016, 2013.
 26. M. Zortea, E. Flores, J. Scharcanski, "A simple weighted thresholding method for the segmentation of pigmented skin lesions in macroscopic images," *Pattern Recogn.*, vol. 64, pp. 92–104, 2017.
 27. Z. Ma, Z., J.M.R.S. Tavares, "A novel approach to segment skin lesions in dermoscopic images based on a deformable model," *IEEE J. Biomed. Health Inf.*, vol. 20, no. 2, pp. 615–623, 2016.
 28. M.E. Celebi, H.A. Kingravi, H. Iyatomi, Y.A. Aslandogan, W.V. Stoecker, R.H. Moss, J.M. Malters, J.M. Grichnik, A.A. Marghoob, H.S. Rabinovitz, S.W. Menzies, "Border detection in dermoscopy images using statistical region merging," *Skin Res. Tech.*, vol. 14, pp. 347–353, 2008.
 29. L. Yu, H. Chen, Q. Dou, J. Qin, P.A. Heng, "Automated melanoma recognition in dermoscopy images via very deep residual networks," *IEEE Trans. Med. Imaging*, vol. 36, no. 4, pp. 994–1004, 2017.
 30. C. Yang, L. Zhang, H. Lu, X. Ruan, M.H. Yang, "Saliency detection via graph-based manifold ranking, in *Proc. IEEE Conf. on Computer Vision and Pattern Recognition*, 2013, pp. 3166–3173.
 31. W. Zhu, S. Liang, Y. Wei, J. Sun, "Saliency optimization from robust background detection," in *Proc. IEEE Conf. on Computer Vision and Pattern Recognition*, 2014, pp. 2814–2821.
 32. M.M. Cheng, N.J. Mitra, X. Huang, P.H.S. Torr, S.M. Hu, "Global contrast based salient region detection," *IEEE Trans Pattern Anal Mach Intell.*, vol. 37, no. 3, pp. 569–582, 2015.
 33. E. Ahn, J. Kim, L. Bi, A. Kumar, C. Li, M. Fulham, D.D. Feng, "Saliency-Based Lesion Segmentation Via Background Detection in Dermoscopic Images," *IEEE J. Biomed. Health Inf.*, vol. 21, no. 6, pp. 1685–1693, 2017.
 34. K. Hu, S. Liu, Y. Zhang, C. Cao, F. Xiao, W. Huang, X. Gao, "Automatic segmentation of dermoscopy images using saliency combined with adaptive thresholding based on wavelet transform", *Multimedia Tools and Applications*, pp. 1–18, 2019.
 35. C. Yang, L. Zhang, H. Lu, X. Ruan, M.H. Yang, "Saliency detection via graph-based manifold ranking, in *Proc. IEEE Conf. on Computer Vision and Pattern Recognition*, 2013, pp. 3166–3173.
 36. W. Zhu, S. Liang, Y. Wei, J. Sun, "Saliency optimization from robust background detection," in *Proc. IEEE Conf. on Computer Vision and Pattern Recognition*, 2014, pp. 2814–2821.
 37. J. Harel, C. Koch, P. Perona, "Graph-Based Visual Saliency," in *NIPS 2006, Advances in Neural Information Processing Systems*, 2007, vol.19, pp. 545–552.
 38. R. Achanta, S. Hemami, F. Estrada, S. Susstrunk, "Frequency-tuned salient region detection", in *Proc. 2009 IEEE Conf. on Computer Vision and Pattern Recognition*, 2009, pp. 1507–1604.

39. Q. Zhang, J. Lin, Y. Tao, W. Li, Y. Shi, "Salient object detection via color and texture cues," *Neurocomputing*, vol. 243, pp. 35–48, 2017.
40. O.O. Olugbara, T.B. Taiwo, D. Heukelman, "Segmentation of melanoma skin lesion using perceptual color difference saliency with morphological analysis", *Mathematical Problems in Engineering*, 2018.
41. A. Dekker, "Kohonen neural networks for optimal colour quantization," *Network Computation in Neural Systems*, vol. 5, no. 3, pp. 351–367, 1994.
42. V. Bruni, G. Ramella, D. Vitulano, "Automatic Perceptual Color Quantization of Dermoscopic Images," in *VISAPP 2015*, J. Braz et al. Eds., Scitepress Science and Technology Publications, vol. 1, 2015, pp. 323-330.
43. G. Ramella, G. Sanniti di Baja, "A new method for color quantization," in *Proc. 12th International Conference on Signal Image Technology & Internet-Based Systems - SITIS 2016*, K. Yetongnon et al. Eds., IEEE Computer Society, 2016, pp. 1-6.
44. T. Mendonca, P.M. Ferreira, J.S. Marques, A.R. Marcal, J. Rozeira, "PH²—A public database for the analysis of dermoscopic images," in *Dermoscopy Image Analysis*, Celebi, M. E., Mendonca, T., Marques, J.S., Eds., Boca Raton, CRC Press, pp. 419-439, 2015. Available: <https://www.fc.up.pt/addi/ph2%20database.html>.
45. ISIC 2016. ISIC Archive: The International Skin Imaging Collaboration: Melanoma Project, ISIC, 5 Jan 2016. [Online]. Available: <https://isic-archive.com/#>.
46. P.M.M. Pereira, R. Fonseca-Pinto, R.P. Paiva, P.A.A. Assuncao, L.M.N. Tavora, L.A. Thomaz, S.M.M.cFaria, "Dermoscopic skin lesion image segmentation based on Local BinaryPattern Clustering: Comparative study," *Biomedical Signal Processing and Control*, vol. 59, 101924, 2020.
47. M. E. Celebi, Y.A. Aslandogan, W.V. Stoecker, H. Iyatomi, H. Oka, X. Chen, "Unsupervised border detection in dermoscopy images," *Skin Res. Tech.*, vol. 13, pp. 454–462, 2007.
48. H. Wang, R. H. Moss, X. Chen et al., "Modified watershed technique and post-processing for segmentation of skin lesions in dermoscopy images," *Computerized Medical Imaging and Graphics*, vol. 35, no. 2, pp. 116–120, 2011.
49. A. Aksac, T. Ozyer, R. Alhaji, "Complex networks driven salient region detection based on superpixel segmentation," *Pattern Recognition*, vol. 66, pp. 268–279, 2017.
50. C. Rother, V. Kolmogorov, A. Blake, "'GrabCut': Interactive foreground extraction using iterated graph cuts," *ACM Trans. Graph.*, vol. 23, no. 3, pp. 309–314, 2004.
51. R. Garnavi, M. Aldeen, M. E. Celebi, A. Bhuiyan, C. Dolianitis, G. Varigos, "Automatic segmentation of dermoscopy images using histogram thresholding on optimal color channels," *Int. J. Medicine and Medical Sciences*, vol. 1, no. 2, pp. 126–134, 2011.
52. M. Zortea, S. O. Skrøvseth, T. R. Schopf, H.M. Kirchesch, F. Godtliebsen, "Automatic segmentation of dermoscopic images by iterative classification," *Int. J. Biomed. Imag.*, vol. 2011, Article ID 972648, 19 pages, 2011.
53. L. Itti, C. Koch, E. Niebur, "A model of saliency-based visual attention for rapid scene analysis," *IEEE Trans. on Patt. Anal. and Mach. Intell.*, vol. 20, no. 11, pp. 1254–1259, 1998.
54. M. R. Guarracino, L. Maddalena, "SDI+: a Novel Algorithm for Segmenting Dermoscopic Images", *IEEE J. Biomed. Health Inf.*, vol. 23, n. 2, pp. 481-488, 2019.
55. D. Gutman, N.C.F. Codella, M.E. Celebi, B. Helba, M. Marchetti, N. Mishra, and A. Halpern, "Skin lesion analysis toward melanoma detection: A challenge at the International Symposium on Biomedical Imaging (ISBI) 2016," hosted by the International Skin Imaging Collaboration (ISIC), arXiv:1605.01397 [cs.CV], 2016.